TEMPORAL ANALYSIS OF THE SOLAR SPECTRUM IN NATAL/RN AND ITS INFLUENCE ON THE PERFORMANCE OF PHOTOVOLTAIC SYSTEMS

Alan Rodrigues de Sousa[12], Samira de Azevedo Santos Emiliavaca[1], Camila Fernanda Cardoso Teixeira[12], Amanda Gomes Barboza[1], Dayane Cynthia Pinto Oliveira[1], Nicholas Medeiros Lopes[12], Gabriela Rocha Alves da Silva[12], Ana Cleide Bezerra Amorim[1], João Vitor Fonseca de Mendonça[1]

[1] SENAI Innovation Institute for Renewable Energy, Natal (Brazil)

[2] Federal University of Rio Grande do Norte, Natal (Brazil)

Abstract

This study analyzes the influence of the spectral distribution of solar irradiance in the city of Natal/RN, a low-latitude region of Brazil, on the performance of photovoltaic technologies. Spectral data measured every minute between 300 and 1100 nm, totaling 33,448 measurements, were synchronized with global horizontal irradiance information from a solarimetric station. The results indicate negligible seasonal variations and a local spectrum enriched in high-frequency components, reflected in Average Photon Energy (APE) values of 1.93 eV, higher than the AM1.5 standard. A comparison between Mono-Si and CdTe modules, using the Spectral Factor (SF), showed greater compatibility of CdTe with the local spectrum, with relative gains of up to 10%, while Mono-Si would have a reduction of up to 4%. These results are similar to those found in the literature for similar latitudes. The high APE values also suggest a greater susceptibility of bifacial modules to Ultraviolet-Induced Degradation (UVID). The results highlight the importance of considering regional spectral conditions and module behavior in real operation, in addition to standard test conditions, for a more accurate assessment of photovoltaic performance.

Keywords: PV performance, Spectral response, APE, Spectral irradiance, Solar irradiance monitoring

1. Introduction

Photovoltaic systems are strongly influenced by their environmental conditions, namely incident irradiance, temperature, and spectral distribution (Minemoto et al., 2009; Sharma and Bhattacharya, 2022). These factors depend on atmospheric and geographic parameters that, in many cases, are quite different from the standard test condition (STC) for which photovoltaic modules are certified (Sirisamphanwong and Ketjoy, 2014; Eke et al., 2017; Minemoto et al., 2009). The conditions for certification are an irradiance of 1000 W/m², a module temperature of 25 °C, and an AM1.5 G spectrum, as defined in IEC 60904-1:2020 and IEC 61215-1:2021. These conditions allow comparisons between the different modules available on the market (Gasparin, Bühler, and Krenzinger, 2012). However, the AM1.5 spectrum is a spectral pattern that represents the distribution of solar radiation after its passage through the Earth's standard atmosphere when the Sun is approximately 48.2° from the zenith. Under real-world conditions, the solar spectrum is altered by atmospheric absorption and scattering due to gases, water vapor, aerosols, and suspended particles. These factors significantly modify the spectral distribution of irradiance, making the AM1.5 spectrum inadequate to accurately represent solar conditions at different photovoltaic system installation locations.

After irradiance, temperature, and soiling, the spectral distribution of radiation is one of the predominant variables affecting the performance of photovoltaic devices in the field (Braga, Do Nascimento, and Rüther, 2019). However, the spectral distribution of radiation is often overlooked in photovoltaic system sizing processes, especially in Brazil, despite several studies demonstrating that, for the same global irradiance value, significant variations in spectral composition can occur (Wang et al., 2023). Furthermore, the mismatch between the spectral response band of existing solar radiometers and the band effectively absorbed by photovoltaic modules can generate significant errors in assessing photovoltaic generation efficiency (Yue et

10.18086/swc.2025.04.47 Available at http://proceedings.ises.org

al., 2024). One characteristic of spectral radiation is related to local latitude: the closer the location is to the equator, the higher the fraction of shorter-wavelength components and the smaller the observed seasonal spectral variations (Sevillano-Bendezú et al., 2023).

The ability of photovoltaic materials to convert solar irradiance into electricity varies with wavelength—that is, the solar spectral selectivity of photovoltaic materials—since only the spectral fraction compatible with this selectivity is effectively converted into energy (Wang et al., 2023). This selectivity is called Spectral Response (SR), which depends on the bandgap, cell thickness, and carrier transport mechanisms. Thus, different photovoltaic technologies exhibit distinct spectral responses depending on the materials and structures used (Ferreira et al., 2012; Haag and Krenzinger, 2014).

Crystalline silicon (c-Si) dominates the photovoltaic market, but new technologies, such as thin-film modules (CdTe, perovskite, and OPV), are gaining prominence. These technologies are more sensitive to the shape of the solar spectrum due to their spectral response. Therefore, the spectral distribution of solar irradiance directly influences the performance of photovoltaic modules. Considering this variability is essential for predicting output power and comparing different technologies. Understanding the solar spectrum is also relevant for emerging applications, such as agrophotovoltaic systems, where the selective absorption properties of plants guide the use of semi-transparent technologies (Ma et al., 2022; Zhang et al., 2023), and hybrid photovoltaic-thermal systems, aiming to optimize the electrical and thermal conversion of radiation (Liew and Lee, 2019; Zhu, Li, and Yu, 2022; Lv et al., 2023). Furthermore, recent results show that modern photovoltaic cell architectures are more vulnerable to UVID compared to conventional cells (Sinha et al., 2023). However, terrestrial spectral databases are still limited and often cover restricted wavelength ranges (Sevillano-Bendezú et al., 2023). This study aims to characterize the local solar spectrum based on field measurements and compare it to the AM1.5 reference spectrum, evaluating the impact of spectral variations on the relative performance of mono-Si and CdTe photovoltaic modules using the spectral factor. The results aim to support the identification of photovoltaic materials best suited to regional spectral conditions, contributing to increased conversion efficiency and the integration of different solar energy applications.

2. Methodology

Global spectral irradiance data were collected during a measurement campaign in Natal, Rio Grande do Norte (latitude -5.824945, longitude -35.226768), at an altitude of 50 meters, from November 2022 to March 2025. The city of Natal has a humid tropical climate, with high temperatures and little variation throughout the year, maintaining averages between 25°C and 30°C. The rainy season occurs between March and July, with April, May, and June being the wettest, while the driest period runs from September to January. Measurements were taken daily between 8:00 AM and 4:00 PM, ensuring a solar elevation angle greater than 20°. This filter minimized the influence of higher air mass (AM) conditions, in which diffuse radiation predominates in global spectral irradiance. Integrated irradiance data exceeding 1600 W/m² were discarded to avoid overirradiance events or spurious measurements.

Spectral irradiance measurements were conducted using a stationary spectroradiometer, model MS-711 from EKO Instruments, as illustrated in Figure 1. The instrument used is a non-collimated hemispherical version, designed for quantifying global spectral irradiance (direct + diffuse components). It is important to note that, in this configuration, the spectroradiometer provides effective spectral irradiance, resulting from a variable mixture of the direct beam radiation and diffuse radiation spectra. This spectral composition is strongly dependent on local atmospheric conditions, such as cloud cover, haze, and solar geometry.

Figure 1: Illustrations of: a) the solarimetric station, b) the MS711 spectroradiometer, and c) a map indicating the study site.

In order to complement the spectral characterization, data from an adjacent solarimetric station, installed less than 5 meters from the spectroradiometer, illustrated in Figure 1, were incorporated. This station provides, in high temporal resolution, measurements every 1 minute of information on global horizontal irradiance (G), direct normal irradiance (Gb), and diffuse horizontal irradiance (Gd), in addition to meteorological variables such as air temperature, relative humidity, wind speed, precipitation, and atmospheric pressure. These parameters were used for a more comprehensive assessment of the prevailing sky conditions during the spectral acquisition periods.

To simplify the analysis of spectral effects on photovoltaic cells, the literature proposes several spectral indices that allow characterizing the incident spectral distribution with a single representative value (Gueymard, 2023). In this study to characterize the solar spectrum of the city of Natal/RN, the APE metric was used, which represents the average energy of photons and describes the spectral distribution of solar irradiance. This is a widely used metric in the photovoltaic community to characterize the spectral quality of irradiance, allowing for the evaluation of how the solar spectrum deviates from standard reference conditions (Norton et al., 2015). The higher the APE, the greater the blue radiation content in sunlight (Nofuentes et al., 2014). It is an instantaneous value defined as the ratio of the total irradiance of the spectrum to the photon flux density (Eke; Betts et al., 2017). Consequently, the definition of APE is generally referred to as a finite integration interval, expressed in the unit of electron-volt (eV) as

$$APE = \frac{\int_{\lambda a}^{\lambda b} G(\lambda) d\lambda}{q_e \int_{\lambda a}^{\lambda b} \Phi(\lambda) d\lambda} \qquad \text{(eq. 1)}$$

where q_e is the electron charge, $\Phi(\lambda)$ is the photon spectral flux density, and λa and λb are the device's absorption wavelength limits.

The APE is an index independent of the photovoltaic device, but highly dependent on the upper and lower limits of spectral integration. For example, the APE for the AM 1.5-G reference spectrum, according to the IEC 60904-3 standard, is 1.88 eV and 1.59 eV for the 350–1050 nm and 350–1700 nm ranges, respectively (Gasparin; Bühler; Krenzinger, 2012). The APE is a widely used parameter to represent the variation in the incident solar spectrum and its potential effects on photovoltaic performance. Complementarily, the spectral factor allows for a more targeted assessment, incorporating the specific spectral response of each technology and more accurately quantifying performance differences compared to the AM1.5G standard spectrum (Sevillano-Bendezú et al., 2023).

To study the influence of the solar spectrum on the performance of Mono-Si and CdTe technologies, the Spectral Factor (SF), also known as the Spectral Mismatch Factor, was used. This factor evaluates the correspondence between the local solar spectrum and the AM1.5 standard, reflecting the conversion efficiency of each technology (Neves et al., 2018). The SF is the factor used to correct discrepancies between measurements of the spectral responses of photovoltaic cells under different solar spectra, known as Spectral

Matching errors. The procedure for correcting the mismatch between the two spectra and the mismatch between SRs of different cells is guided by the following equation taken from the IEC 60904-7:2019 standard.

$$SF = \frac{\int E_{ref}(\lambda)d\lambda}{\int E_{meas}(\lambda)d\lambda} \frac{\int E_{meas}(\lambda)SR(\lambda)d\lambda}{\int E_{ref}(\lambda)SR(\lambda)d\lambda} = \frac{I_{meas}}{I_{ref}} \frac{E_{ref}}{E_{meas}} \quad \text{(eq. 2)}$$

where, E_{ref}, E_{meas}, SR, I_{meas}, I_{ref} are, the reference spectral irradiance, the measured spectral irradiance, the spectral response of the cell, the measured current and the reference current, respectively.

3. Results and Discussion

3.1. Spectral Distribution

The irradiance spectral distributions, obtained in the wavelength range from 300 to 1100 nm and recorded every minute by a spectroradiometer, totaling 33,448 measurements after data filtering, indicated that the spectral composition of solar radiation in the city of Natal, Rio Grande do Norte, exhibits insignificant seasonal variations and high-frequency components. Figure 2 presents the average monthly spectral distribution for the period from November 2022 to March 2025, along with the AM1.5 reference spectrum and the average spectrum observed during the analyzed period. Figure 3 shows that the spectral distribution for the city of Natal, Rio Grande do Norte, exhibits higher intensities in the blue region and lower intensities in the red and green regions, indicating that the APE index is higher than that of the AM1.5 standard spectrum.

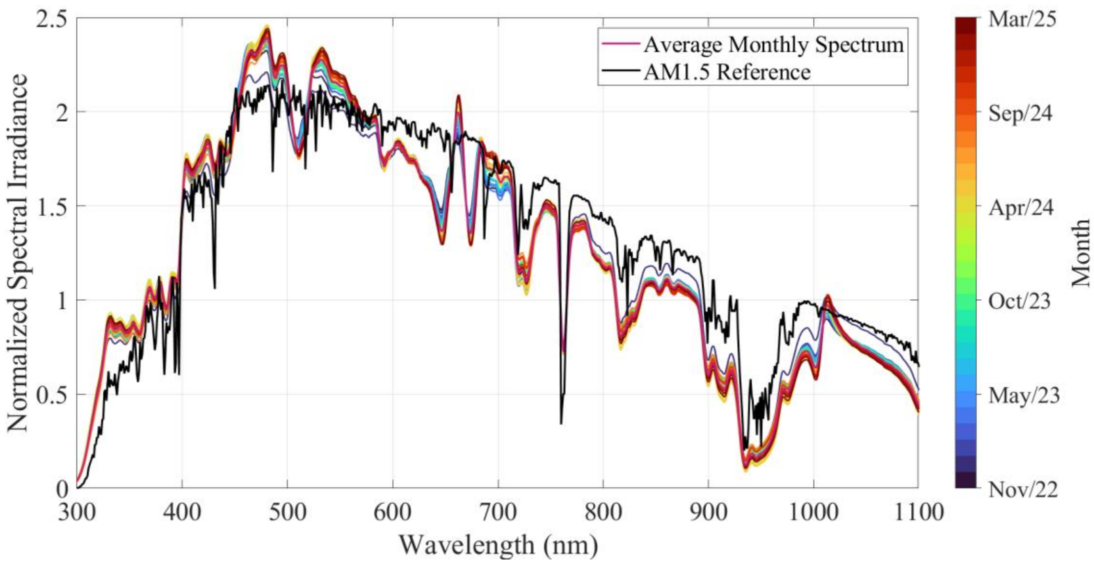

Figure 2: Monthly average spectral distribution compared with the AM1.5 reference spectrum and the mean of the measured spectrum.

The normalized spectral contribution by band of the measured distributions is presented in Figure 3, which shows the average value of the spectral distribution contribution in 50 nm intervals. It can be observed that the values remain close throughout the year, even considering the seasonality of the measurements. Figure 4 shows the difference between the measured spectra and the standard spectrum, showing the deviations for each frequency band. In the 350, 400, and 450 nm bands, the measured spectra showed higher intensities of approximately 20%, 12%, and 4%, respectively, compared to the AM1.5 spectrum. On the other hand, in the 800 to 1100 nm band, the measured values were significantly lower, reaching about 70% at 950 nm, when compared to AM1.5.

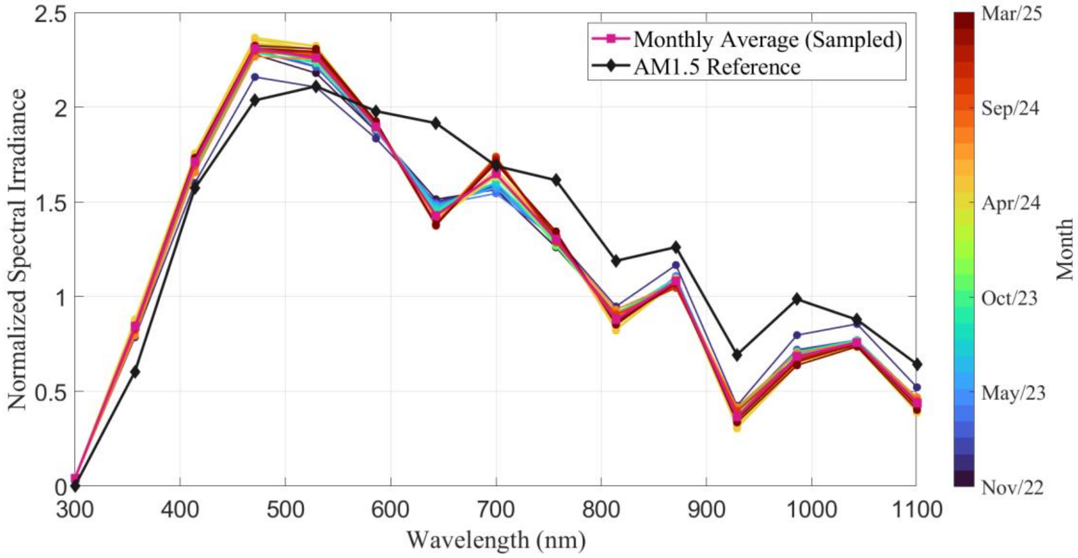

Figure 3: Mean contribution of the local spectral irradiance distribution, computed in 50 nm wavelength intervals over the measurement period.

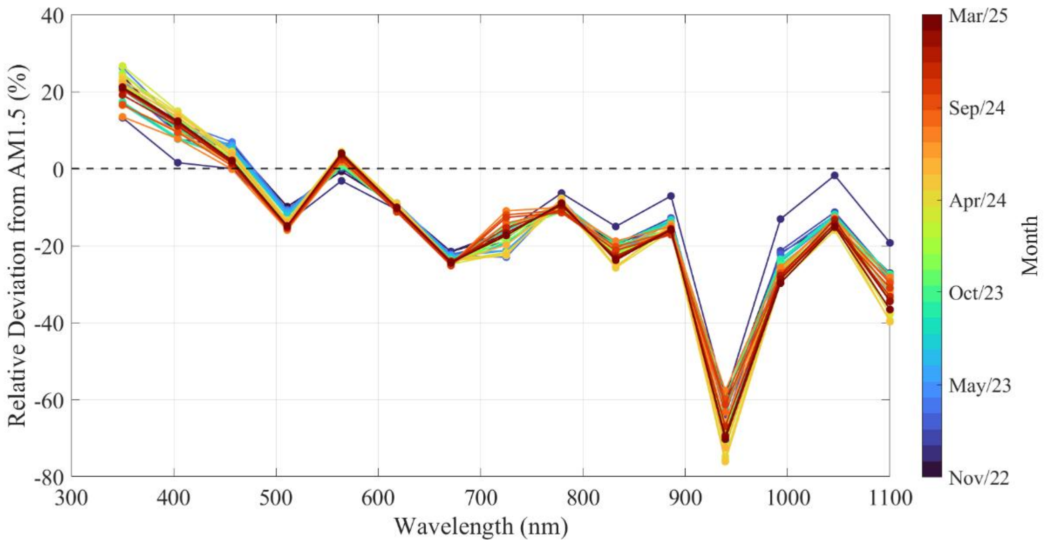

Figure 4: Deviations between the measured spectra and the standard reference spectrum, illustrating the variations across the spectral bands.

3.2. Comparison of Measurements

The APE values for the set of 33,448 measurements were calculated using Equation 1 for the range of 300 to 1100 nm. The values demonstrate a constant APE index with few seasonal variations and a value higher than that of the standard AM 1.5 solar spectrum. Figure 5 illustrates the seasonal variation of the average monthly spectrum, corroborating the results of Sevillano-Bendezú et al. (2023), which indicate that, in low-latitude locations, the spectrum tends to present a higher APE index and reduced seasonal variations. The month with the highest average APE value of 1.946 eV was April 2024, while December 2022 presented the lowest APE of 1.895 eV.

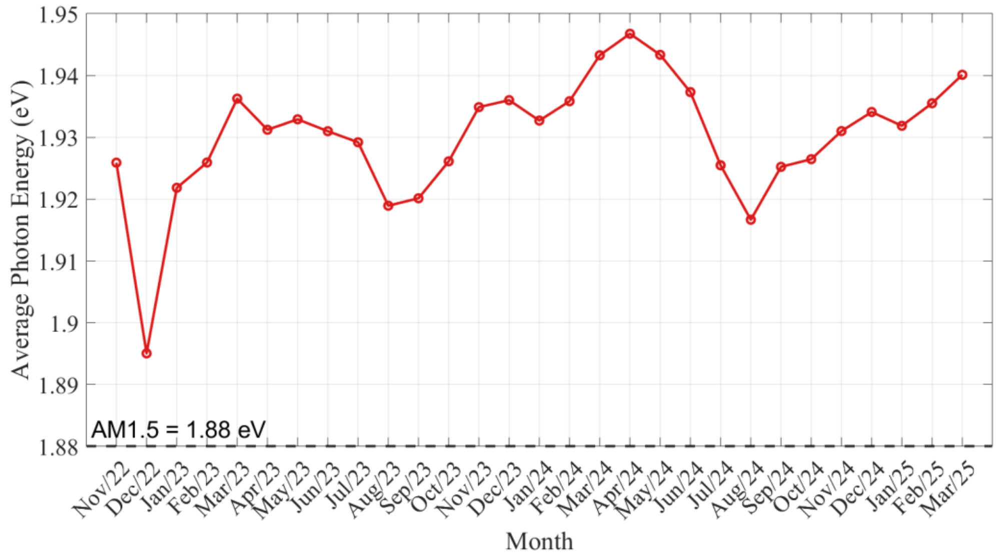

Figure 5: Variation of APE over Months.

The statistical results of the APE index over the measurement period indicate an average of 1,930 eV, with a standard deviation of 0.036 eV, revealing relative stability of the spectrum over time. Values ranged from 1,663 eV to 2,339 eV, with the first and third quartiles located at 1,912 eV and 1,942 eV, respectively. These results show that, overall, the solar spectrum in Natal, Rio Grande do Norte, presents a high energy content, with a predominance of higher-energy photons. This is reinforced by the presence of APE values above the standard average (1,878 eV for AM1.5), indicating a greater incidence of shorter-wavelength radiation. These results are in agreement with those presented by Emiliavaca and Sousa (2025) where average APE values of 1.912 eV were found for the month of July 2021, also in the city of Natal. Table 1 summarizes the main statistics of the data.

Table 1: Statistical summary of APE index values observed during the analysis period.

APE (eV)	Samples	Percent (%)	Mean	Std_dev	Min	Max
1.6-1.8	139	0.416	1.697	0.023	1.664	1.691
1.8-2.0	31764	94.965	1.927	0.024	1.809	1.921
2.0-2.2	1538	4.598	2.034	0.032	2.000	2.024
> 2.2	7	0.021	2.269	0.046	2.223	2.259

To correlate the APE index values with global irradiance, the data measured by the spectroradiometer were synchronized with the irradiance measurements obtained by the solarimetric station. Figure 6 shows the relationship between APE and G for irradiance values greater than 600 W/m², showing that all measurements resulted in APE indices above 1.88 eV, a value corresponding to the AM1.5 reference spectrum. Another relevant aspect is the tendency for APE values to concentrate around 1.93 eV, regardless of the irradiance intensity. Even under high irradiance conditions, reaching up to 1502 W/m², the APE index remained at 1.90 eV, thus remaining above the typical AM1.5 value. This greater intensity in the shorter wavelength bands (blue region) may contribute to the UVID effect in installed photovoltaic modules, especially in modern technologies that are more sensitive to ultraviolet radiation, as demonstrated in the work of Sinha et al. (2023).

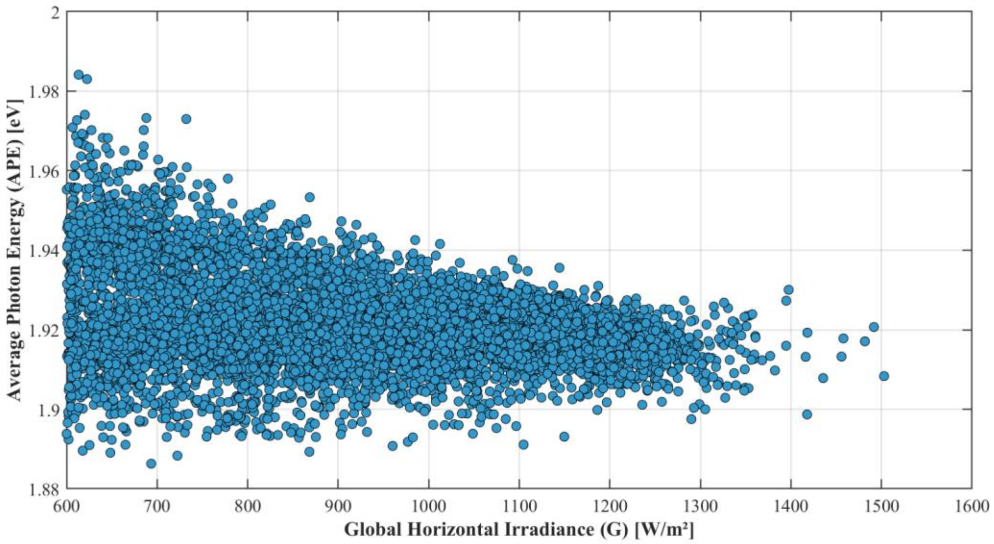

Figure 6: Relationship between APE and global horizontal irradiance (G) at the measurement location.

The highest APE value recorded during the analysis period for the city of Natal occurred on December 15, 2023 (Figure 7a), at 8:30 am, reaching 2.259 eV with an irradiance of 461.98 W/m². On the other hand, the lowest APE value was observed on February 12, 2025 (Figure 7b), at 1:23 pm, with 1.664 eV and an irradiance of 867.77 W/m². Figure 7 presents the irradiance profiles corresponding to these two days, evidencing atmospheric conditions with high cloudiness and precipitation. It can be observed that the day with the highest APE recorded 70.1 mm of rainfall, while the day with the lowest APE presented only 3.3 mm of precipitation. These results indicate that the presence of dense clouds and intense rainfall events are associated with greater dispersion of solar radiation, leading to a spectrum richer in short wavelengths, resulting in higher APE values.

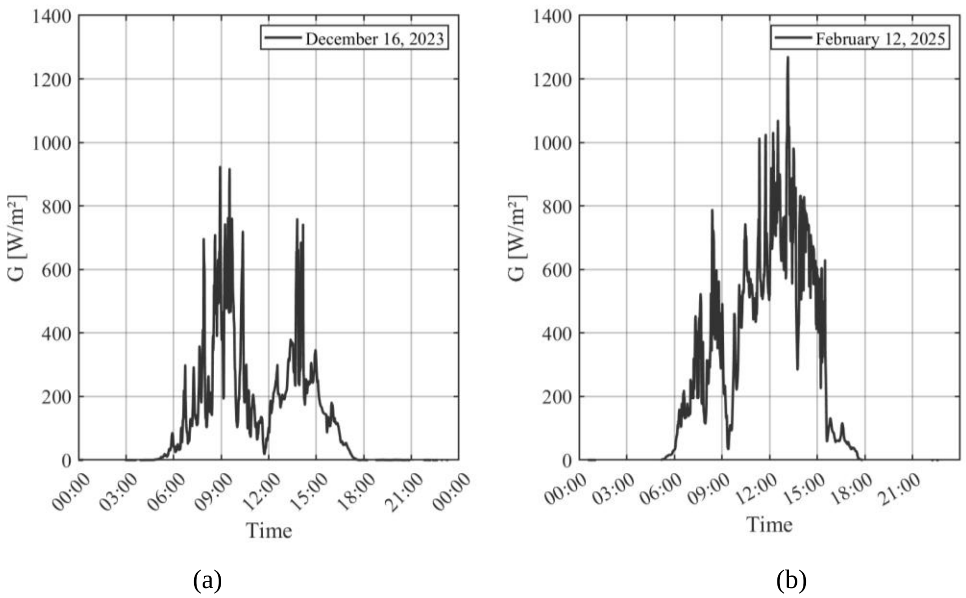

Figure 7: Comparison of daily radiation on the days presenting the highest and lowest APE indices during the measurement period.

3.3. Spectral Gain

To analyze the influence of the measured spectrum on two photovoltaic technologies (CdTe and Mono-Si), the EF was used to compare the expected performance differences between the technologies. Figure 8 presents the monthly average spectral factor by technology, showing that the EF for Mono-Si technology is less than 1, approximately 0.96, while for CdTe it is greater than 1, around 1.1. This result was expected, since CdTe technology exhibits better efficiency when the spectrum is rich in high-frequency components.

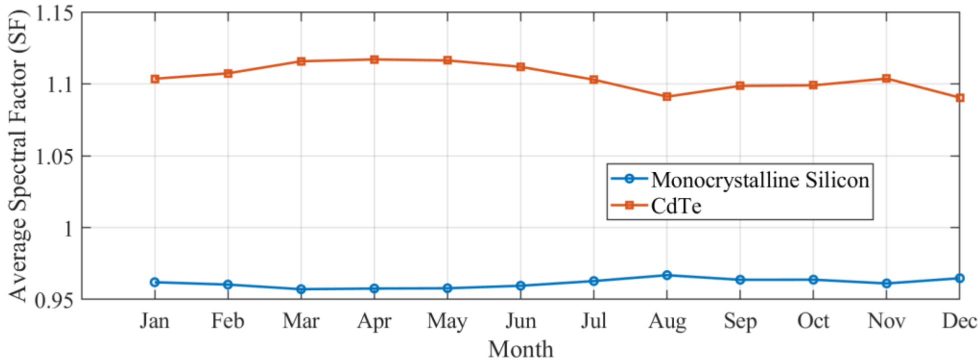

Figure 8: Monthly average spectral factor for each PV technology.

The relative spectral gain (CdTe vs. Mono-Si) showed values greater than 1 throughout all months, as illustrated in Figure 9, indicating that CdTe technology has better compatibility with the local solar spectrum compared to Mono-Si. A seasonal variation in this gain is also observed, with progressively higher values between March and May, a period in which the spectrum has a higher content in the blue/UV range. This characteristic favors CdTe, whose spectral response is more efficient in this region, unlike mono-Si, which has a broader response and is less sensitive to spectral variations.

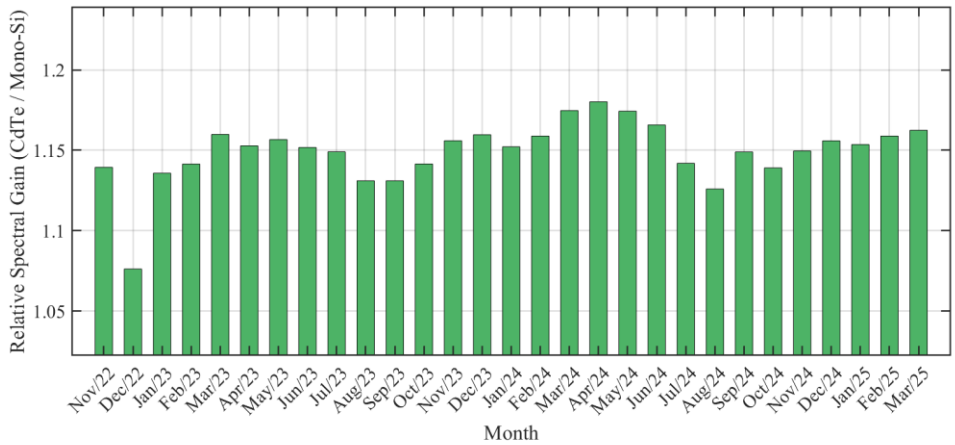

Figure 9: Monthly spectral gain of CdTe relative to mono-Si.

The results obtained indicate that, in the Natal/RN region, irradiance presents a high concentration of high-frequency components, corroborating the trend observed by Sevillano-Bendezú et al. (2023), who estimated an average annual APE of approximately 1.92 eV for latitudes close to 10°. Extrapolating to latitudes around 5°, the APE index would be close to 1.925 eV, a value quite close to the 1.93 eV obtained in this study. Furthermore, the findings are consistent with those reported by Braga, Do Nascimento, and Rüther (2019), in which CdTe modules showed spectral gains of about 10% in regions close to the one studied. These results reinforce the conclusion of Lv et al. (2023) that spectral effects can alter photovoltaic performance by up to 6%, depending on the geographic location.

4. Conclusion

The analysis of the spectral data shows that the local solar spectrum exhibits insignificant seasonal variations throughout the year, a behavior typical of low-latitude regions. The APE calculation confirmed that the local spectrum is enriched in high-frequency components, presenting a significant spectral difference compared to the AM1.5 reference standard. This result reinforces the trend observed in low-latitude regions, which typically exhibit higher APE values. This discrepancy indicates that the spectrum incident on the photovoltaic modules differs substantially from that used under standard test conditions, directly impacting the performance of field-installed photovoltaic systems. The CdTe-based photovoltaic technology showed superior spectral gains, indicating better compatibility with the local solar spectrum compared to Mono-Si technology. Similar results for CdTe gain have been reported in the literature for locations near Natal, Rio Grande do Norte.

Additionally, the high APE values suggest that photovoltaic modules with newer technologies, especially bifacial ones installed in the region, may be more susceptible to the effects of UVID. This result reinforces the need for specific investigations into the impact of this degradation under field conditions. Furthermore, the findings highlight the importance of regional spectral studies for optimization and technology selection, suggesting that the classification of photovoltaic modules should consider their energy yield under real-world irradiance, temperature, and spectral distribution conditions, rather than relying solely on the power measured under standard test conditions.

5. Acknowledgments

Research work carried out in the context of the activities of the National Institute for Technological Development of Photovoltaic Solar Energy Applications, INCT-DAESF, CNPq/MCTI/Brazil, Process 408486/2024-4. The authors thank the SENAI Institute for Innovation in Renewable Energy for the support and infrastructure provided, CTG Brasil for the financial contribution under the ANEEL PD-10381-0620/2020 project, and TotalEnergies for the current financial contribution under the ANP 23980-6 and ANP 24118-2 projects.

6. References

Braga, M., do Nascimento, L.R., & Rüther, R. (2019). Spectral modeling and spectral impacts on the performance of mc-Si and new generation CdTe photovoltaics in warm and sunny climates. *Solar Energy*, 188, 976–988.

de Azevedo Santos Emiliavaca, S., & Rodrigues de Sousa, A. (2025). Análise do espectro da radiação solar na cidade de Natal-RN. *Revista Brasileira De Energia Solar*, 16(1), 28–38.

Eke, R., Betts, T.R., et al. (2017). Spectral irradiance effects on the outdoor performance of photovoltaic modules. *Renewable and Sustainable Energy Reviews*, 69, 429–434.

Ferreira, T.A., et al. (2012). Sistema para caracterização espectral de dispositivos fotovoltaicos. *Revista Brasileira de Energia Solar*, 3, 47–53.

Gasparin, F.P., Bühler, A.J., & Krenzinger, A. (2012). Análise da importância do fator de descasamento espectral na caracterização elétrica de módulos fotovoltaicos. *Revista Brasileira de Energia Solar*, 3(2), 94.

Gueymard, C.A. (2023). Assessment of the global applicability of three leading indices that characterize the spectral distribution of solar irradiance impacting various photovoltaic technologies. *Energy Conversion and Management*, 295, 117602.

IEC (2020). *IEC 60904-1: Photovoltaic (PV) modules – Part 1: Measurement of current-voltage characteristics*. Geneva: International Electrotechnical Commission.

IEC (2021). *IEC 61215-1: Crystalline silicon terrestrial photovoltaic (PV) modules – Design qualification and type approval – Part 1: Test requirements*. Geneva: International Electrotechnical Commission.

Liew, N.J.Y., & Lee, H.-J. (2019). Numerical analysis of hybrid photovoltaic-thermal systems utilizing different spectral bandpass filters. *Renewable Energy*, 144, 15–29.

Lv, S., et al. (2023). Comparative analysis of photovoltaic thermoelectric systems using different photovoltaic cells. *Applied Thermal Engineering*, 235, 121356.

Ma, Q., et al. (2022). Photovoltaic/spectrum performance analysis of a multifunctional solid spectral splitting covering for passive solar greenhouse roof. *Energy Conversion and Management*, 251, 114955.

Minemoto, T., et al. (2009). Uniqueness verification of solar spectrum index of average photon energy for evaluating outdoor performance of photovoltaic modules. *Solar Energy*, 83(8), 1294–1299.

Neves, G.M., et al. (2018). Influência do espectro solar em módulos fotovoltaicos sob céu limpo, céu parcialmente nublado e céu nublado. In: *Anais do Congresso Brasileiro de Energia Solar (CBENS)*.

Nofuentes, G., et al. (2014). Analysis of the dependence of the spectral factor of some PV technologies on the solar spectrum distribution. *Applied Energy*, 113, 302–309.

Norton, M., Amillo, A.M.G., & Galleano, R. (2015). Comparison of solar spectral irradiance measurements using the average photon energy parameter. *Solar Energy*, 120, 337–344.

Sevillano-Bendezú, M.A., et al. (2023). Predictability and interrelations of spectral indicators for PV performance in multiple latitudes and climates. *Solar Energy*, 259, 174–187.

Sharma, M.K., & Bhattacharya, J. (2022). Dependence of spectral factor on angle of incidence for monocrystalline silicon based photovoltaic solar panel. *Renewable Energy*, 184, 820–829.

Sinha, A., et al. (2023). UV-induced degradation of high-efficiency silicon PV modules with different cell architectures. *Progress in Photovoltaics: Research and Applications*, 31(1), 36–51.

Sirisamphanwong, C., & Ketjoy, N. (2012). Impact of spectral irradiance distribution on the outdoor performance of photovoltaic system under Thai climatic conditions. *Renewable Energy*, 38(1), 69–74.

Wang, S., et al. (2023). Evaluation of the energy conversion performance of different photovoltaic materials with measured solar spectral irradiance. *Renewable Energy*, 219, 119431.

Yue, C., et al. (2024). New models of solar photovoltaic power generation efficiency based on spectrally responsive bands. *Applied Energy*, 375, 123936.

Zhang, Z., et al. (2023). Spectral-splitting concentrator agrivoltaics for higher hybrid solar energy conversion efficiency. *Energy Conversion and Management*, 276, 116567.

Zhu, T., Li, Q., & Yu, A. (2022). Analysis of the solar spectrum allocation in a spectral-splitting photovoltaic-thermochemical hybrid system. *Solar Energy*, 232, 63–72.